Thermal stability and data retention of resistive random access memory with HfO_x/ZnO double layers*

Yun-Feng Lai(赖云锋)†, Fan Chen(陈凡), Ze-Cun Zeng(曾泽村), Pei-Jie Lin(林培杰), Shu-Ying Cheng(程树英), and Jin-Ling Yu(俞金玲)

School of Physics and Information Engineering, Fuzhou University, Fuzhou 350108, *China*

(Received 23 March 2017; revised manuscript received 15 May 2017; published online 20 June 2017)

As an industry accepted storage scheme, hafnium oxide (HfO_x) based resistive random access memory (RRAM) should further improve its thermal stability and data retention for practical applications. We therefore fabricated RRAMs with HfO_x/ZnO double-layer as the storage medium to study their thermal stability as well as data retention. The HfO_x/ZnO double-layer is capable of reversible bipolar switching under ultralow switching current (< 3 μA) with a Schottky emission dominant conduction for the high resistance state and a Poole–Frenkel emission governed conduction for the low resistance state. Compared with a drastically increased switching current at 120 °C for the single HfO_x layer RRAM, the HfO_x/ZnO double-layer exhibits excellent thermal stability and maintains neglectful fluctuations in switching current at high temperatures (up to 180 °C), which might be attributed to the increased Schottky barrier height to suppress current at high temperatures. Additionally, the HfO_x/ZnO double-layer exhibits 10-year data retention @85 °C that is helpful for the practical applications in RRAMs.

Keywords: resistive random access memory (RRAM), thermal stability, data retention, double layer

PACS: 73.40.Rw, 77.80.Fm, 65.60.+a **DOI:** 10.1088/1674-1056/26/8/087305

1. Introduction

As one of the most promising nonvolatile storage technologies exhibiting fast write/read speed, good scalability, low power consumption, and good endurance, resistive random access memory (RRAM) has attracted much attention from industries and academic communities.[1–4] In recent years, various metal oxides have been studied as the storage medium of RRAMs, and conducting models have been adopted to interpret the oxide-based resistive switching.[4–10] Among them, hafnium oxide (HfO_x) has been intensively investigated for its approbation from industries. Shrinking physical dimensions of a memory cell to meet the requirements of three-dimensional (3D) integration is an inevitable choice for further expanding the storage capability and meeting the demand of neuromorphic computing.[5,11–13] However, tiny space accommodating cells in a large number would face fluctuations in switching parameters due to the thermal disturbance triggered by joule-heating. Consequently, the significance of improving thermal stability and data retention is manifest.[14–17]

In order to achieve this goal, several schemes have been attempted.[18–22] Keeping the density of oxygen vacancy (V_o) high enough has been confirmed to effectively ensure thermal stability and data retention.[18,19] If a more thermally-stable thin film serves as a cap to suppress oxygen releasing from active switching layers, the thermal stability and data retention might also be enhanced due to the maintenance of V_o.[20] Additionally, metal electrodes with suitable thermodynamic ability are able to strengthen the thermal stability and data retention of an RRAM by forming conductive filaments with favorable geometry to alleviate oxygen stochastic movements.[21] Furthermore, a buffer layer could also be used to sustain the stability of a V_o assisted conductive filament (CF).[22] Therefore, sustaining the status of the V_os (or oxygen ions) is critical for improving thermal stability and data retention, and the thin films adjacent to the active switching layers may play an important role.

As wide band gap oxides exhibit high transmittance in visible regions, HfO_x and zinc oxide (ZnO) with excellent switching properties have also been considered as the storage medium of a transparent RRAM.[14,23–27] Several schemes have been proposed to enhance switching properties. However, few efforts have been made to improve thermal stability and data retention. As we know, electron barrier at the interface might affect the switching properties of an RRAM, whose thermal stability and data retention might be affected as well. Recently, we have reported switching current reduction with an HfO_x/ZnO double-layer,[28] confirming effects of interface on performance. However, thermal stability and data retention are still absent. In this paper, we further investigate the HfO_x/ZnO double-layer (DL) to study the effects of the adjacent ZnO layer on the thermal stability and data retention of the RRAMs.

*Project supported by the National Natural Science Foundation of China (Grant Nos. 61006003 and 61674038), the Natural Science Foundation of Fujian Province, China (Grant Nos. 2015J01249 and 2010J05134), the Science Foundation of Fujian Education Department of China (Grant No. JAT160073), and the Science Foundation of Fujian Provincial Economic and Information Technology Commission of China (Grant No. 83016006).

†Corresponding author. E-mail: yunfeng.lai@fzu.edu.cn

© 2017 Chinese Physical Society and IOP Publishing Ltd

2. Experimental details

To fabricate an HfO_x/ZnO double-layer RRAM as shown in the inset of Fig. 1(a), procedures were the same as presented in Ref. [28]. All depositions were completed at room temperature. The RRAMs with single layer (SL) (Ti/∼15 nm ZnO/ITO and Ti/∼30 nm HfO_x/ITO) were also fabricated for comparisons. The as-fabricated memory cells were subsequently tested with a semiconductor parameter analyzer (4200-SCS; Keithley, USA) with 0.5 V for reading resistance. Voltage bias was applied on the top electrode (TE) while the bottom electrode (BE) was kept electrically grounded. The measurements were carried out at room temperature to 180 °C in order to evaluate the thermal stability and data retention. The composition of the thin films was also studied by an x-ray photoelectron spectrometer (XPS, Escalab 250; Thermo Scientific, USA) equipped with a monochromatic Al Kα source ($h\nu = 1486.60$ eV). Scans with a step of 0.05 eV and pass energy of 30 eV were performed for binding energies of specific elements with charge correction using the C 1s spectra at 284.60 eV.

3. Results and discussion

3.1. Switching properties of the RRAMs

Figure 1(a) shows the DC swept current–voltage (I–V) curves of the SL-RRAMs and the DL-RRAM. Forming-free and bipolar resistive switching (RS) behaviors are observed from the multi-cycled I–V curves. The DL-RRAM switches from an initial high resistance state (HRS) to a low resistance state (LRS) with a compliance current (I_{cc}) of ∼ 2 μA to avoid hard breakdown, and the set process is thus completed by a low power of ∼ 14 μW. For the reset process to complete the transformation from an LRS to an HRS, ∼ 0.8 μW (100 nA, −8 V) is required. Consequently, the HfO_x/ZnO double-layer suppresses switching current to μA from mA. Another obvious feature of the DL-RRAM is the asymmetric I–V curves. Considering the symmetric I–V curves of the SL-RRAMs [Figs. 1(a), 1(c), and 1(d)], the asymmetric I–V curves may be ascribed to the barrier at the HfO_x/ZnO interface.[29,30] Additionally, uniformity of set voltage is improved by the HfO_x/ZnO double-layer with suppressed fluctuations. To evaluate the thermal stability of the switching properties, we investigated the temperature dependence of the set voltage and the set current from room temperature to 180 °C. As shown in Fig. 2, increasing ambient temperatures decreases the set voltages to less than 5 V for both the DL-RRAM and the SL-RRAM. As for the set current to complete the transformation from an HRS to an LRS, the DL-RRAM sustains a low switching current (∼ 2 μA) with neglectful fluctuations at ambient temperatures up to 180 °C, while the set current of the SL-RRAM abruptly increases at temperatures over 120 °C [see Fig. 2(b)].

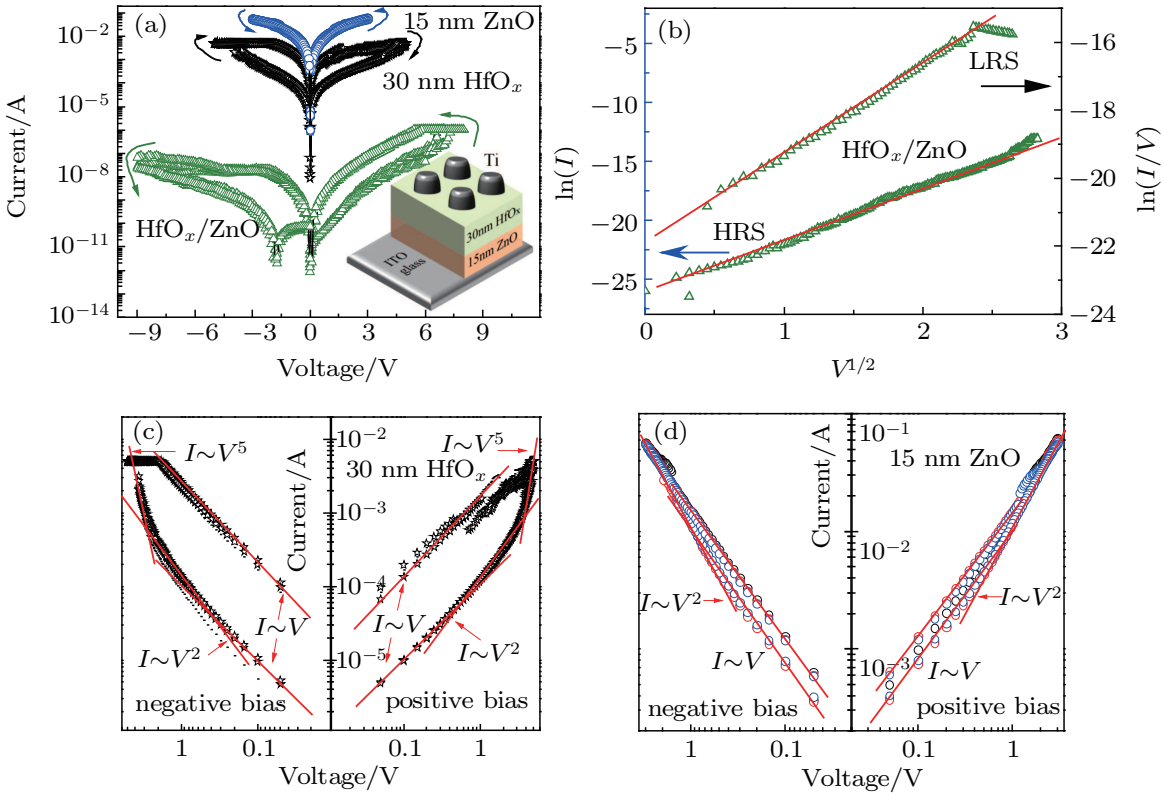


Fig. 1. (color online) (a) Reproducible I–V curves of the SL-RRAMs and DL-RRAM with the device structural diagram in the inset, (b) $\ln(I)$–$V^{0.5}$ and $\ln(I/V)$–$V^{0.5}$ fittings for the HRS and LRS of the DL-RRAM. Also, double logarithmic scale I–V curves of the SL-RRAMs with (c) 30-nm HfO_x and (d) 15-nm ZnO are present.

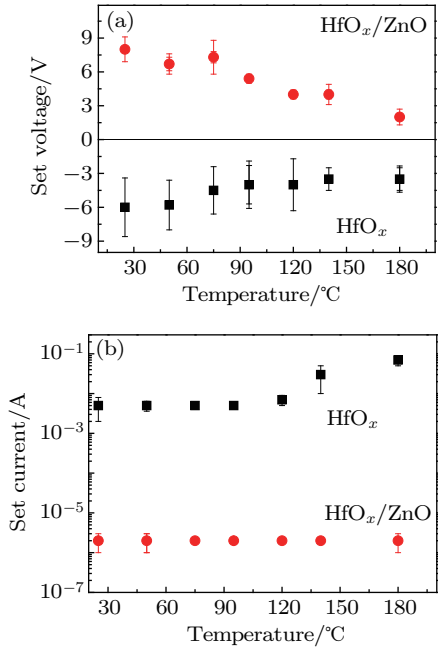


Fig. 2. (color online) Temperature-dependence of (a) set voltage and (b) set current of the DL-RRAM and the 30-nm HfO_x-based SL-RRAM.

3.2. Switching mechanism of the RRAMs

As shown in Fig. 3, the currents at both the HRS and the LRS increase with temperature rise, which excludes electrons transportation through metallic conductive filaments but suggests a semiconductor conduction behavior.[31] Several mechanisms have been proposed to explain conductions during switches, the fittings of the measured I–V curves using different conduction mechanisms such as Schottky emission, Poole–Frenkel, Fowler–Nordheim, and space charge limited current (SCLC) behavior, have been carried out.[32] The well linear fittings of the $\ln(I) \sim V^{0.5}$ and the $\ln(I/V) \sim V^{0.5}$ shown in Fig. 1(b) respectively suggest a Schottky emission dominant conduction in the HRS and a Poole–Frenkel emission governed conduction in the LRS. However, the double logarithmic scale I–V curves of the SL-RRAMs shown in Figs. 1(c) and 1(d) indicate SCLC-dominant conductions for the HRS due to the integration of an Ohmic region (I–V), a Child's square-law region (I–V^2), and even a region with exponentially increased current (I–V^5). As for the LRS of the SL-RRAMs, the presented Ohmic behaviors suggest a filament-assisted conduction. Therefore, the applied electric field in an initial HRS SL-RRAM usually drives oxygen ions out of the lattice matrix and leaves V_os to form CFs to complete the normally observed transformation from an HRS to an LRS.[31]

To highlight the switching mechanism in the DL-RRAM, oxygen migration should be taken into account. Once the HfO_x layer is deposited on the ZnO layer, the oxygen ions in the ZnO thin film would migrate into the HfO_x thin film due to a difference in Gibbs free energy of oxide formation ($\Delta G_{f,ZnO} = -320.5$ kJ/mol and $\Delta G_{f,HfO_x} = 1145.0$ kJ/mol),[20,22] which results in a more conductive ZnO layer with many more V_os and a more electrically insulative HfO_x layer with more stoichiometric properties. To confirm this hypothesis, we prepared thick (~ 30 nm) HfO_x films on glass substrate, thick (~ 30 nm) HfO_x films on the ZnO layer, and thin (~ 5 nm) HfO_x films on the ZnO layer. O 1s XPS spectra of the three samples were then acquired as shown in Fig. 4. An ignorable peak shifting can be observed for the two thick HfO_x films, while an obvious O 1s peak shifting to lower values appears for the thin HfO_x films on the ZnO layer, suggesting oxygen release from the ZnO layer creates a less oxygen-deficient HfO_x layer and leaves the ZnO layer with many more V_os.[20] Therefore, the ZnO layer in an as-prepared DL-RRAM is indeed highly conductive which also agreed with what was observed in Figs. 1(a) and 1(d). To complete electron transport from the BE to the TE, conduction band offset (CBO) acting as barrier (2.35 ± 0.02 eV) at the HfO_x/ZnO interface should thus be overcome,[28] exhibiting a Schottky emission dominant conduction in the HRS as shown in Fig. 1(b).[28,30]

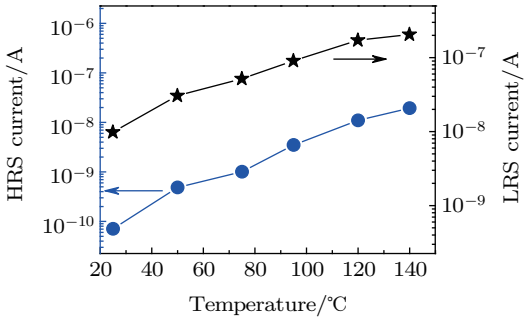


Fig. 3. (color online) Temperature-dependent currents @0.5 V for the HRS and LRS of the DL-RRAMs.

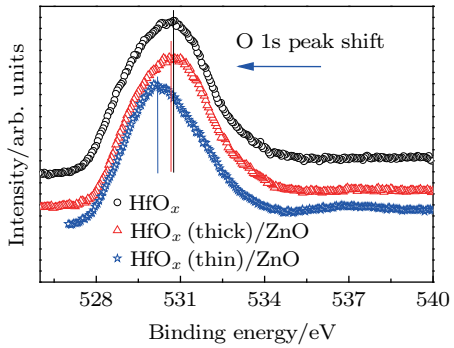


Fig. 4. (color online) O 1s XPS spectra of the HfO_x thin films and those deposited on the ZnO.

If further increased electric field is applied to the memory cell to complete the set process, some V_os in the HfO_x thin film would be generated to serve as trapping centers for electron transportation.[28] Unlike the V_os in the ZnO with a high concentration to form conductive channels, V_os in the HfO_x thin film are still insufficient for electron direct transport between them. Considering the increased electric field to reduce Coulomb potential energies of the electrons, the probability of an electron getting into the conduction band of the HfO_x thin

film by thermal excitation out of the trapping centers (V_os in the HfO_x thin film) would be increased.[32] Therefore, we can observe the Poole–Frenkel emission conduction in the LRS, whose current density (J_{LRS}) is thus given by[33]

$$\ln(J_{LRS}/E) = q(k_BT)^{-1}\sqrt{qE/\pi\varepsilon_r\varepsilon_0} - q(k_BT)^{-1}\varphi_t + \ln C = A(T)\sqrt{E} + B(T), \quad (1)$$

where T is the temperature, k_B is the Boltzmann constant, q is the electric charge, E is the electric field, ε_0 is the permittivity of free space, ε_r is the relative dielectric permittivity, φ_t is the barrier height for electron emission from the trapping center, C is constant, and $B(T) = -q(k_BT)^{-1}\varphi_t + \ln C$ represents the ordinates intercepts of the extension line in the graph of $\ln(J_{LRS}/E)$ against $E^{0.5}$ [see Fig. 5(a)]. The emission barrier height (φ_t) could thus be acquired according to the slope of $B(T)$ versus $1000/T$ as shown in Fig. 5(b), which is agreed with the trapping energy of V_o in α-HfO_x.[34] The conduction in the LRS could thus be governed by a Poole–Frenkel emission mechanism with the V_os assisting electron transport in the HfO_x.

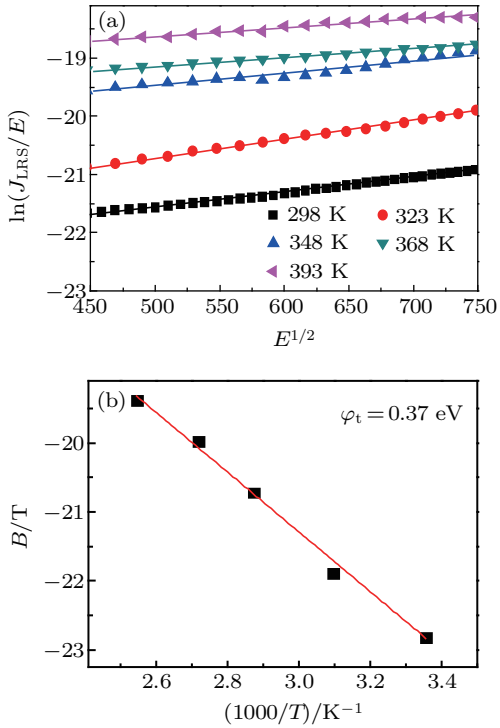


Fig. 5. (color online) (a) $\ln(J_{LRS}/E)$–$E^{0.5}$ curves of the LRS of the DL-RRAM at different temperatures, and (b) the intercepts $B(T)$ obtained from the curves in panel (a) as a function of $1000/T$.

3.3. Understanding the thermal stability and data retention

Thermal stability of the switching current is very important for maintaining normal working status at high temperatures. The Schottky emission dominant conduction in the HRS suggests a close relationship between the current and the Schottky barrier height (Φ_B). We therefore investigated the temperature-dependence of Schottky barrier height of the DL-RRAMs.

Increased temperature may facilitate oxygen ions getting out of lattice matrix by leaving V_os in the oxides. For the SL-RRAM under an electric field, more V_os would be generated at high temperatures to favor the formation of V_o assisted conductive filament. Consequently, we observe a drastically increased current at high temperatures as shown in Fig. 2(b). However, situations would be totally different for the DL-RRAMs.[28] As the oxide-deficient HfO_x exhibits p-type conduction behavior and the presence of V_os normally causes n-type ZnO,[35,36] a p–n junction forms at the HfO_x/ZnO interface. According to the band diagram of the DL-RRAMs,[28] a more p-type HfO_x with a more upward band bending and a more n-type ZnO with a more downward band bending might be formed at the HfO_x/ZnO interface due to the generation of V_os under high temperature. Conduction band offset (CBO) acting as Φ_B at the HfO_x/ZnO interface should thus be increased to sustain ultralow switching current at even 180 °C as what was observed in Fig. 2(b). Apart from the above discussion, experimental results also confirm the hypothesis. The current density at the HRS (J_{HRS}) can be determined by the Schottky emission:[37]

$$J_{HRS} = A^*T^2\exp[-q(\Phi_B - \sqrt{qE/4\pi\varepsilon_r\varepsilon_0})/k_BT], \quad (2)$$

where A^* is the Richardson constant, Φ_B is the Schottky barrier height, and the other parameters are previously defined. At a certain temperature, Φ_B can be expressed as $\Phi_B = k_BTq^{-1}[\ln(A^*T^2) - \ln J_{HRS0}]$ where J_{HRS0} means the current density at the temperature if the electric field is zero. We could thus plot $\ln(J_{HRS})$–$E^{0.5}$ curves for the HRS at different temperatures as shown in Fig. 6, according to which the $\ln J_{HRS}$ changes less than 10 upon the temperature variations from 298 K to 393 K. Considering the room temperature CBO ($\sim$ 2.35 eV) of the HfO_x/ZnO layer,[28] the barrier heights at the HfO_x/ZnO interface would thus be reduced to $\sim$ 2.43, $\sim$ 2.61, $\sim$ 2.74, and 2.91 eV respectively for 323, 348, 368 and 393 K, indicating the Φ_B actually increases with the rising of temperature.

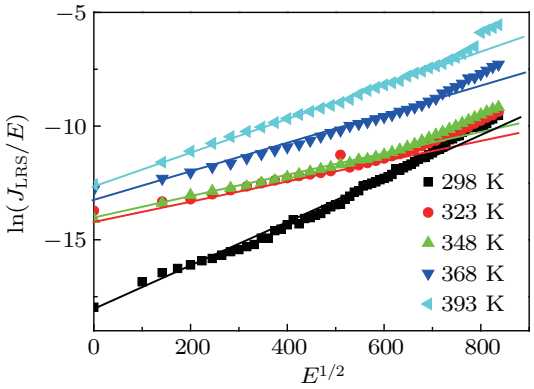


Fig. 6. (color online) $\ln(J_{HRS})$–$E^{0.5}$ curves of the HRS of the DL-RRAM at different temperatures.

Data retention is also crucial for the practical applications of the RRAMs. To investigate the retention reliability of the RRAMs, the thermal accelerating measurement for resistance switching under various temperatures was carried out. Figure 7 shows the data retentions of the DL-RRAMs and the SL-RRAMs at different temperatures. The retention failure time was defined as the time for the resistance increasing to twice of its original value (@LRS) or decreasing to half of its original value (@HRS). According to the retention failure times present in Fig. 7, the HfO_x/ZnO layers extend the HRS retention failure time at all temperatures, suggesting desirable HRS retention characteristic with the HfO_x/ZnO double layers. For the LRS, the HfO_x/ZnO layers shorten the retention failure time to 600 s from 2500 s at 180 °C, but prolong it to 9800 s from 8900 s at lower temperature of 160 °C, indicating the HfO_x/ZnO double layers might favor LRS data retention at lower temperatures. To further estimate the retention characteristic, we plotted the mean retention failure time versus the reciprocal temperature as shown in Fig. 8, which presents the data retention ability of resistance states by using the Arrhenius equation. This equation is expressed as $t_{\text{failure}} \propto \exp(-E_a/k_B T)$, where t_{failure} is the retention time, E_a is the activation energy for the oxygen ions diffusion or V_o migration, k_B and T are Boltzmann's constant and the ambient temperatures, respectively.[38,39] The retention lifetime of the RRAM could be obtained by an extraction result of the Arrhenius equation. Therefore, the HfO_x/ZnO double layers stabilize the 85-°C HRS retention time to be ∼ 10 years instead of 159 hours for the SL-RRAM. Additionally, the 85-°C LRS retention of the DL-RRAM could also be extended to be more than 10 years from 78 hours of the SL-RRAM.

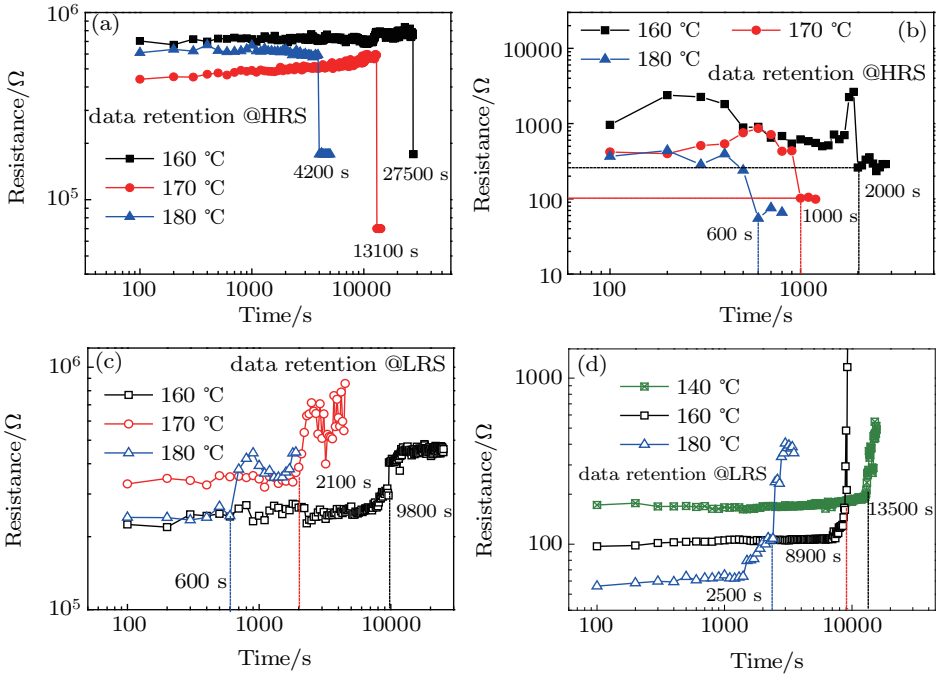


Fig. 7. (color online) Data retention at different temperatures for [(a) and (c)] the DL-RRAM and [(b) and (d)] the SL-RRAM.

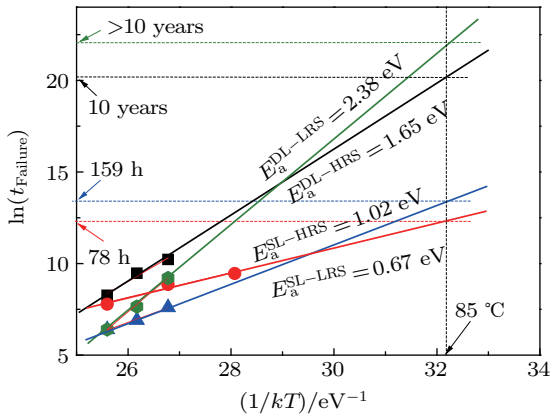


Fig. 8. (color online) Temperature-dependence of the retention failure times and their fitting lines following the Arrhenius equation for the DL-RRAM- and the 30-nm HfO_x-based SL-RRAMs.

Retention failure should be associated with redistribution of V_os to affect electron transport and device resistance. As previously discussed, the V_os assisted CFs would be responsible for the LRS conduction in an HfO_x-based SL-RRAM, instead of the V_os sparsely distributing to assist electron transport governed by a Poole–Frenkel emission conduction in a DL-RRAM. Driven by the concentration gradient, oxygen ions easily move to CFs and combine with V_os to narrow or even cut off CFs. Therefore, the redistribution of the V_os in an SL-RRAM usually exhibits obvious resistance changes. As for the DL-RRAMs, redistribution of V_os might also be affected by temperature rise. However, since the V_os in the HfO_x are sparsely and topologically distributed, slight stochastic move-

ment of the V_os is able to secure electron transport with neglectful variations in resistance. Consequently, resistance variations of the LRS SL-RRAM would be more sensitive to temperature rise than that for an LRS DL-RRAM as shown in Fig. 8.

When it comes to the HRS data retention, the formation of V_os is obviously necessary to be responsible for the retention failure. A rise in temperature produces V_os in both the DL-RRAMs and the SL-RRAMs, which favors the formation of a conductive filament in the SL-RRAMs and results in an HRS retention failure. However, once V_os generate in the HfO_x thin films of an HRS DL-RRAM, it might be filled with some oxygen ions migrating from the ZnO layer, as ZnO has a greater Gibbs free energy of oxide formation than HfO_x. The HfO_x/ZnO double layers could thus hold a better HRS data retention than a single HfO_x layer.

4. Conclusions

The sputter-deposited HfO_x/ZnO double-layer capable of reversible bipolar switching has been prepared with a Schottky emission dominant conduction in the HRS and a Poole–Frenkel emission governed conduction in the LRS. Switching current of the DL-RRAMs can be sustained at high temperatures (up to 180 °C) with neglectful fluctuations, which is ascribed to the increase of Schottky barrier height at the HfO_x/ZnO interface to suppress the increase of current at high temperatures. In addition, the HfO_x/ZnO double-layer shows no less than 10 years of data retention for the HRS and the LRS.

References

[1] Chang T C, Chang K C, Tsai T M, Chu T J and Sze S M 2016 *Mater. Today* **19** 254
[2] Jeong D S, Thomas R, Katiyar R S, Scott J F, Kohlstedt H, Petraru A and Hwang C S 2012 *Rep. Prog. Phys.* **75** 076502
[3] Waser R, Dittmann R, Staikov G and Szot K 2009 *Adv. Mater.* **21** 2632
[4] Yang J J, Inoue I H, Mikolajick T and Hwang C S 2012 *MRS Bull.* **37** 131
[5] Yu S, Chen H Y, Gao B, Kang J and Wong H S P 2013 *ACS Nano* **7** 2320
[6] Lee M J, Lee C B, Lee D, Lee S R, Chang M, Hur J H, Kim Y B, Kim C J, Seo D H, Seo S, Chung U I, Yoo I K and Kim K 2011 *Nat. Mater.* **10** 625
[7] Deng N, Pang H and Wu W 2014 *Chin. Phys. B* **23** 107306
[8] Jiang R, Du X H, Han Z Y and Sun W D 2015 *Acta Phys. Sin.* **64** 207302 (in Chinese)
[9] Gao B, Sun B, Zhang H W, Liu L F, Liu X Y, Han R Q, Kang J F and Yu B 2009 *IEEE Electron Dev. Lett.* **30** 1326
[10] Gao B, Kang J F, Liu L F, Liu X Y and Yu Bin 2011 *Appl. Phys. Lett.* **98** 232108
[11] Burr G W, Shenoy R S, Virwani K, Narayanan P, Padilla A, Kurdi B and Hwang H 2014 *J. Vac. Sci. Technol. B* **32** 23
[12] Hsu C W, Hou T H, Chen M C, Wang I T and Lo C L 2013 *IEEE Electron Dev. Lett.* **34** 885
[13] Gao B, Bi Y, Chen H Y, Liu R, Huang P, Chen B, Liu L, Liu X, Yu S, Wong H S P and Kang J 2014 *ACS Nano* **8** 6998
[14] Shang J, Liu G, Yang H, Zhu X, Chen X, Tan H, Hu B, Pan L, Xue W and Li R W 2014 *Adv. Funct. Mater.* **24** 2171
[15] Puglisi F M, Qafa A and Pavan P 2015 *IEEE Electron Dev. Lett.* **36** 244
[16] Walczyk C, Walczyk D, Schroeder T, Bertaud T, Sowinska M, Lukosius M, Fraschke M, Wolansky D, Tillack B, Miranda E and Wenger C 2011 *IEEE Trans. Electron Dev.* **58** 3124
[17] Chen C, Song C, Yang J, Zeng F and Pan F 2012 *Appl. Phys. Lett.* **100** 253509
[18] Ninomiya T, Wei Z, Muraoka S, Yasuhara R, Katayama K and Takagi T 2013 *IEEE Trans. Electron Dev.* **60** 1384
[19] Cabout T, Vianello E, Jalaguier E, Grampeix H, Molas G, Blaise P, Cueto O, Guillermet M, Nodin J F, Perniola L, Blonkowski S, Jeannot S, Denorme S, Candelier P, Bocquet M and Muller C 2014 *Proceedings of the IEEE 6th International Memory Workshop (IMW)*, May 18–21 Taipei, Taiwan, pp. 1–4
[20] Chand U, Huang K C, Huang C Y, Ho C H, Lin C H and Tseng T Y 2015 *J. Appl. Phys.* **117** 184105
[21] Chen Y Y, Goux L, Clima S, Govoreanu B, Degraeve R, Kar G S, Fantini A, Groeseneken G, Wouters D J and Jurczak M 2013 *IEEE Trans. Electron Dev.* **60** 1114
[22] Chand U, Huang C Y and Tseng T Y 2014 *IEEE Electron Dev. Lett.* **35** 1019
[23] Simanjuntak F M, Panda D, Tsai T L, Lin C A, Wei K H and Tseng T Y 2015 *J. Mater. Sci.* **50** 6961
[24] Simanjuntak F M, Panda D, Tsai T L, Lin C A, Wei K H and Tseng T Y 2015 *Appl. Phys. Lett.* **107** 033505
[25] Yu H, Kim M, Kim Y, Lee J, Kim K K, Choi S J and Cho S 2014 *Electron. Mater. Lett.* **10** 321
[26] Kim A, Song K, Kim Y and Moon J 2011 *ACS Appl. Mater. Interfaces* **3** 4525
[27] Yan X B, Hao H, Chen Y F, Li Y C and Banerjee W 2014 *Appl. Phys. Lett.* **105** 093502
[28] Lai Y F, Zeng Z C, Liao C H, Cheng S Y, Yu J L, Zheng Q and Lin P J 2016 *Appl. Phys. Lett.* **109** 063501
[29] Chen Q, Yang M, Feng Y P, Chai J W, Zhang Z, Pan J S and Wang S J 2009 *Appl. Phys. Lett.* **95** 162104
[30] Lu H L, Yang M, Xie Z Y, Geng Y, Zhang Y, Wang P F, Sun Q Q, Ding S J and Zhang D W 2014 *Appl. Phys. Lett.* **104** 161602
[31] Lai Y F, Xin P C, Cheng S Y, Yu J L and Zheng Q 2015 *Appl. Phys. Lett.* **106** 031603
[32] Chiu F C 2014 *Adv. Mater. Sci. Eng.* **2014** 578168
[33] Arslan E, Butun S and Ozbay E 2009 *Appl. Phys. Lett.* **94** 142106
[34] Chen T J and Kuo C L 2014 *Microelectron. Reliab.* **54** 1119
[35] Hildebrandt E, Kurian J, Muller M M, Schroeder T, Kleebe H J and Alff L 2011 *Appl. Phys. Lett.* **99** 112902
[36] Liu L S, Mei Z X, Tang A H, Azarov A, Kuznetsov A, Xue Q K and Du X L 2016 *Phys. Rev. B* **93** 235305
[37] Park J, Biju K P, Jung S, Lee W, Lee J, Kim S, Park S, Shin J and Hwang H 2011 *IEEE Electron Dev. Lett.* **32** 476
[38] Wu M C, Lin Y W, Jang W Y, Lin C H and Tseng T Y 2011 *IEEE Electron Dev. Lett.* **32** 1026
[39] Park J, Jo M, Bourim E M, Yoon J, Seong D J, Lee J, Lee W and Hwang H 2010 *IEEE Electron Dev. Lett.* **31** 485